RHIC Lattice for Electron Cooling

Introduction

The current geometry of the RHIC interaction region (IR) must be modified to accommodate the requirements for electron cooling. The requirements are:

1. Moderate β functions of 50 *m* for injection acceptance.
2. Large β functions of 400 *m* through the electron cooling region.
3. Vertical beam separation of 7 *cm* at the interaction point (IP).

To achieve these goals we need to modify the existing RHIC IR. In the sections that follow, we present a proposal on necessary modifications to achieve the above requirements.

Geometry

To provide enough drift space, we present a local and global geometric solution. First, consider a global approach that involves two IRs. Here we will untwists both IP12 and IP4 [1], see Figs 1 and 2. This is proposed so that one IR will be used for eCooling and a the other IR is used for eRHIC.

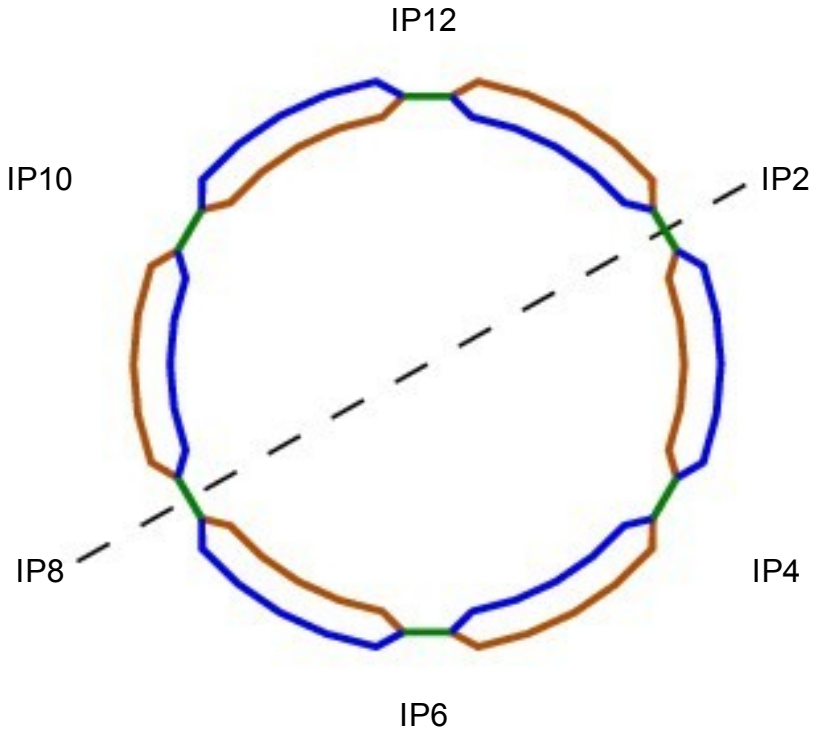

Figure 1: Schematic of RHIC layout for both Blue and Yellow rings with six independent interaction regions.

The problem with this approach is the cost. At IP2 the Blue beam will be passing through a Yellow sector and vice versa. In these sectors many of the magnets will need to have there polarity changed which will be an expensive undertaking. For this reason a local approach has been proposed.

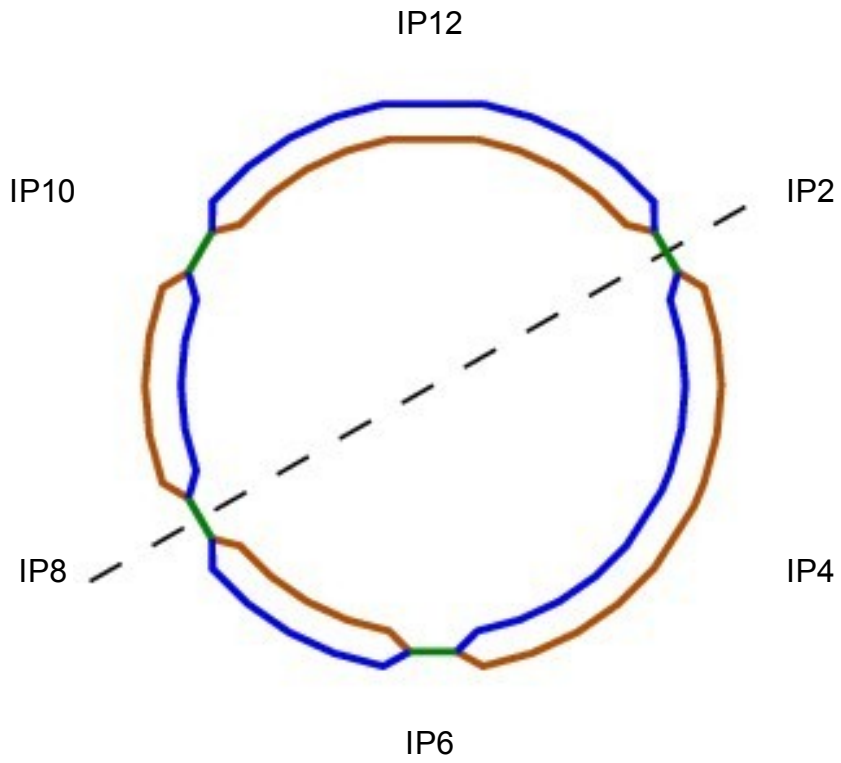

Figure 2: Schematic of RHIC interaction regions with IP12 and IP4 untwisted. With this proposal, one IR can be used for electron cooling while the other IR can be used for eRHIC.

In the local approach, only one IR is modified [2]. The crossing dipoles are removed and the strengths for the D5 magnets are adjusted so the beams continue through their respective rings. Fig 3 shows a schematic of this proposal. The change in geometry causes this insertion to be shorter by 1.996 *mm* than the standard RHIC insertion.

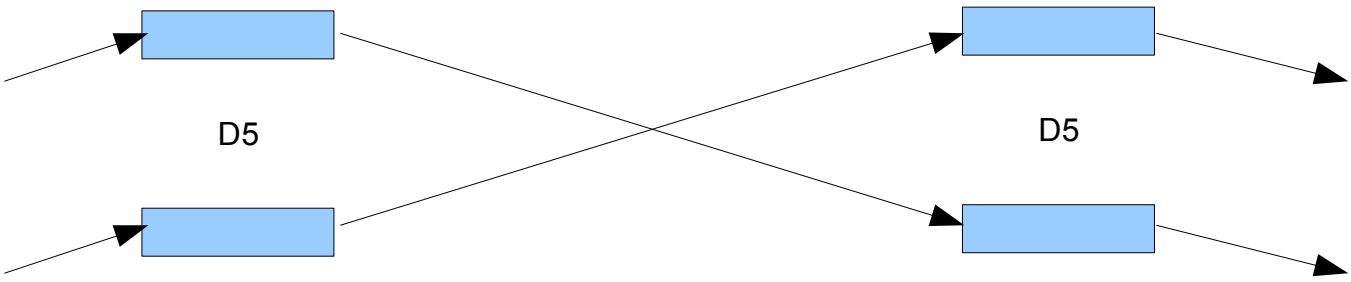

Figure 3: Schematic for changing only one IR. This approach provides enough drift space to meet the electron cooling requirements. Since the beams can still cross, vertical separation will be required to prevent this.

For cost reasons we adopt the local approach. In the next section we discuss the beam optics.

Optics

The goal for the optics is to provide a large β function in both planes through a large warm drift space. This β function should be 400 *m*. Furthermore, we would like to reuse as much existing hardware as

possible to reduce the overall cost. Without the crossing dipoles, the triplets can be moved much further from the IP providing a large drift space for the electron cooling. Additionally, we will not be using the quadrupoles Q4 and Q5. Due to the need of a large current in the outer Q6, this is replaced with the longer Q4 magnet. The calculated currents assume this change.

To find a solution, there is a minimum of 12 constraints as shown in the schematic Fig 4.

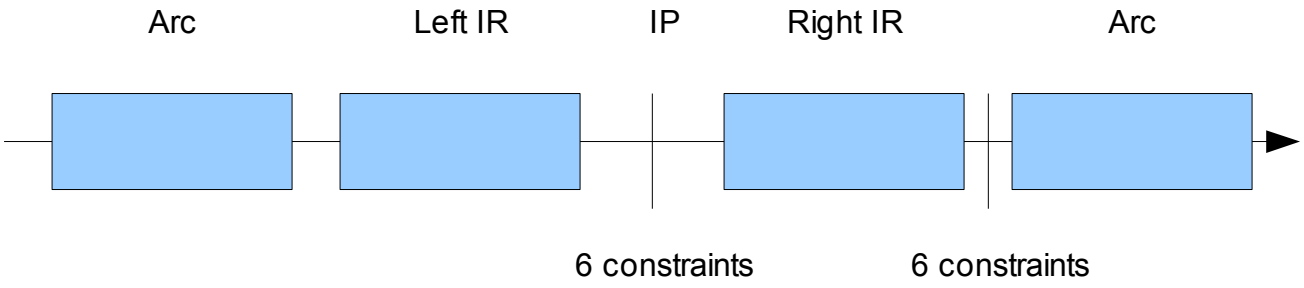

Figure 4: Schematic showing the minimum of 12 constraints used in the matching. Six constraints at the IP to achieve the large β functions desired and 6 more constraints to match the insertion to the arcs. Additional constraints for controlling the β functions in the IR sections are also used.

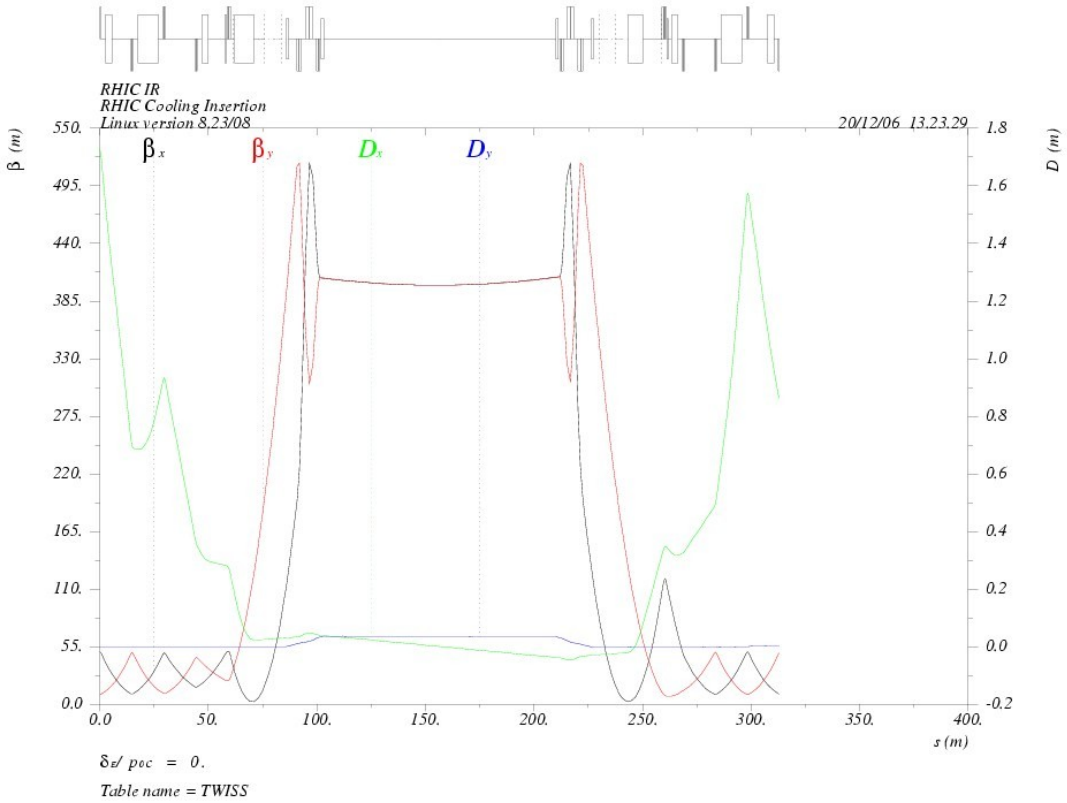

Figure 5: The twiss and dispersion functions for the electron cooling section with a 400*m* β functions through the large warm drift space.

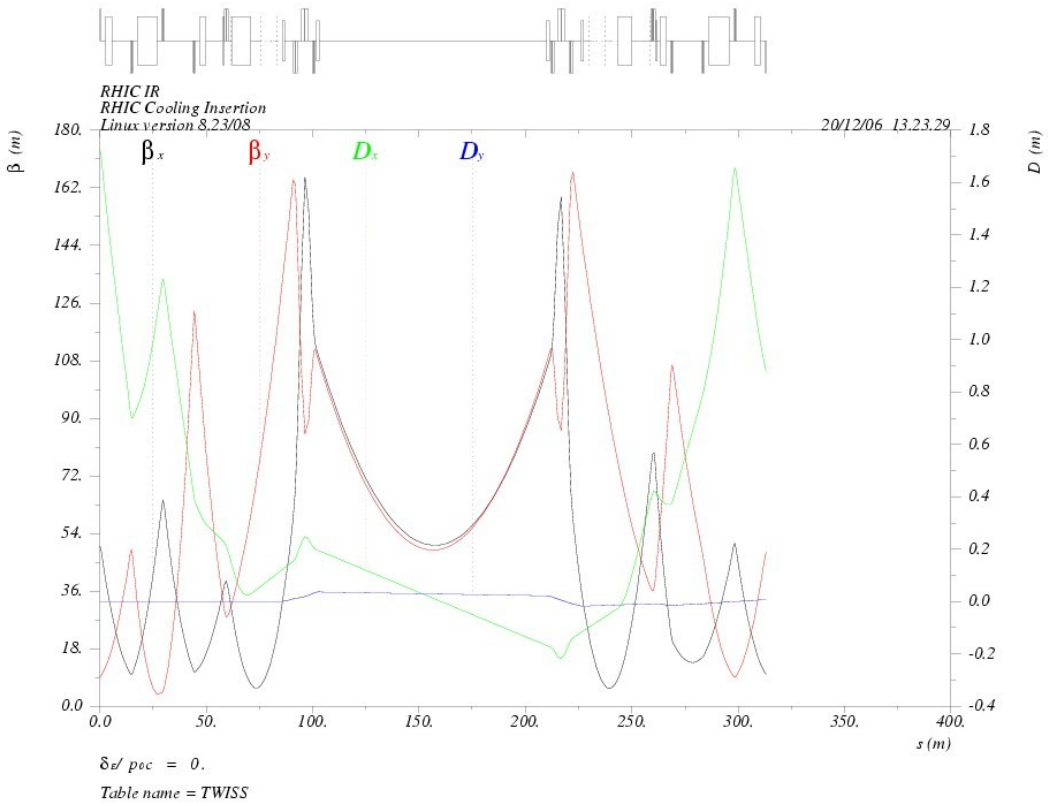

Figure 6: The twiss and dispersion functions for the electron cooling section with a 50*m* β functions through the large warm drift space. For injection optics.

The optics matching is performed using the MAD program [3]. Fig. 5 shows the twiss and dispersion for optics with 400 *m* through the electron cooling region.

Since the β function is large, injection acceptance needs to be addressed. To allow sufficient acceptance, a 50 *m* β insertion is desired. Furthermore, a smooth squeeze path of the power supplies from 50 *m* to 400 *m* is required. Fig. 6 shows the optics for the 50 *m* β solution. Fig. 7 shows the quadrupole gradients as a function of β. All other quadrupoles and dipoles beyond the D5 magnets remain unchanged except the Q6O was replaced by a Q4 magnet which is longer resulting in the quadrupole center further from the IP and Q6I magnet was moved 6.226 *m* away from the IP.

In the next section, we look at the hardware requirements.

Magnets

The D5 dipoles are connected to the main dipole bus in RHIC. The strengths of these dipoles must be changed in order for the beam line to go from a D5 magnet to the other D5. Note, there are two D5 magnet types: an inside type and an outside type. The change in strengths required are shown in Table 1.

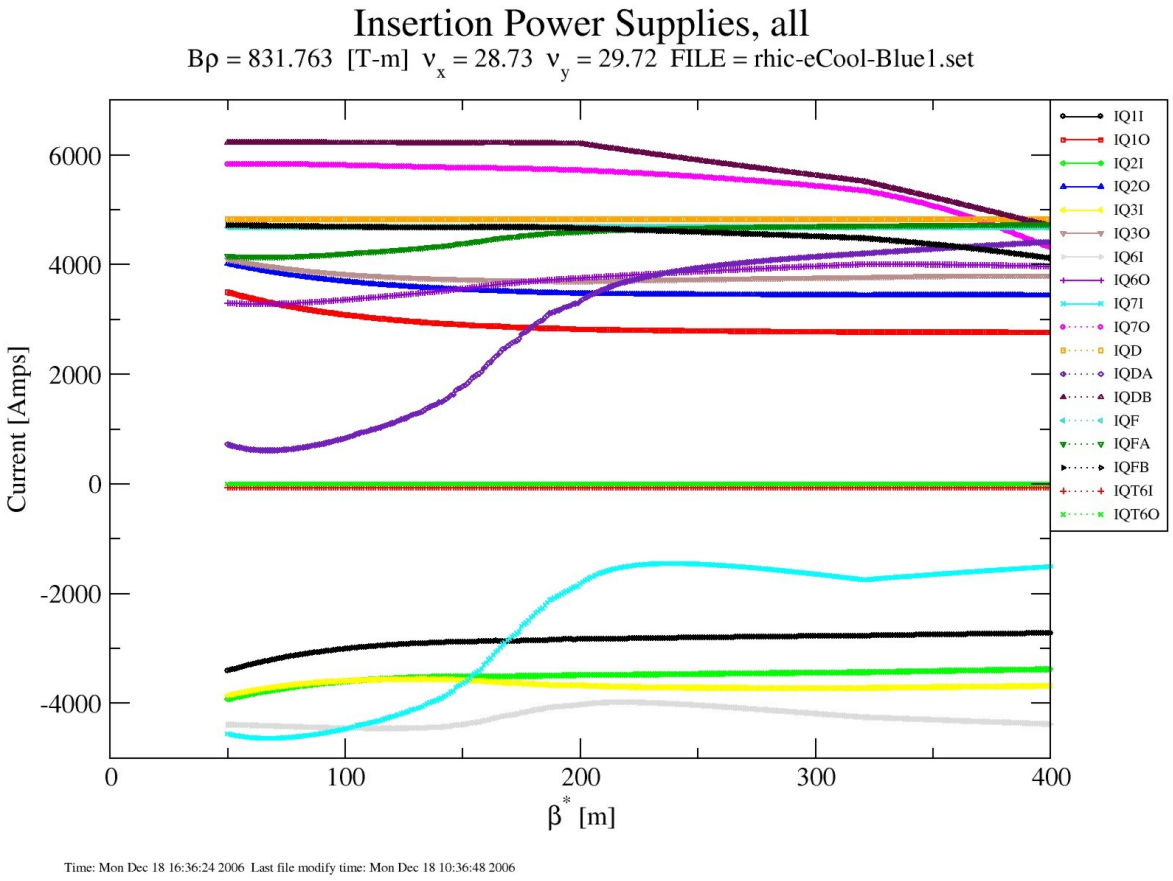

Figure 7: The gradients of the quadrupoles (Bρ = 831.763*T-m*) versus the insertion β function. This is for the blue ring eCooling section. The gradients for the yellow eCooling section differs slightly from the blue ring.

Table 1: The change in bend angle for the inner, D5I, and outer, D5O, D5 dipoles.

Dipoles	Length [m]	Current Angle [mrad]	Change in Angle [mrad]	Change
D5O	8.698	35.863893	1.320244	3.6813%
D5I	6.916	28.514816	-1.320244	-4.6300%

This can be handled by adding a shunt power supply on these magnets.

For the quadrupoles, we present their corresponding strengths and estimate the current required. These results are shown in Tables 2 and 3 for the heavy ion and proton electron cooling sections.

In these solutions the Q6 magnets, both inner and outer are quite strong. Since, the Q4 quadrupole, which is longer than Q6, is not being used, we can replace the Q6 with Q4 to reduce the current requirements. In Table 3, we need to keep an eye on Q9O and Q7O quadrupoles, which also require large currents.

Table 2: The strengths and estimated currents with 400 *m* β function. Note, the longer length of Q6O comes from using an Q4 which is no longer used. Furthermore, 70 *Amps* current is in the trim quadrupole next to the Q6I to reduce its strength.

Quad	Gradient [T/m]	Strength [m^-2]	Length [m]	Current [kA]
Q9O	-70.17	-0.08437	1.110	-4.703
Q8O	61.61	0.07407	1.110	4.119
Q7O	-64.35	-0.07737	0.930	-4.307
Q6O	59.57	0.07161	1.812	3.966
Q3O	-36.16	-0.04348	2.100	-3.796
Q2O	32.75	0.03937	3.392	3.435
Q1O	-26.34	-0.03166	1.440	-2.762
Q1I	-25.95	-0.03120	1.440	-2.721
Q2I	32.24	0.03876	3.392	3.382
Q3I	-35.13	-0.04224	2.100	-3.687
Q6I	65.47	0.07871	1.110	4.381
Q6I-trim	22.10	0.02657	0.750	0.070
Q7I	-22.59	-0.02716	0.930	-1.511
Q8I	-65.93	-0.07927	1.110	-4.412
Q9I	70.60	0.08488	1.110	4.732

Vertical Separation Bumps

The vertical separation of the 'blue' and 'yellow' crossing rings was designed without affecting the existing horizontal solution of [~110 *m* long cooling interaction region with the β_x~400 *m* high betatron function throughout]. The vertical dispersion matching is accomplished by the simplest possible solution with the four small vertical bending magnets. Four magnets per ring, 1.1 *m* long, are identical, and placed right before and after the triplet cryostat. The crossing point at the center of the interaction region needs to have two rings vertically separated. The vertical separation at the crossing region is 7 *cm*. This is satisfying very much the aperture limitations set up in RHIC because the sigma of the beam is $\sigma = \sqrt{\frac{(\epsilon_N/\pi)\beta_y}{6(\gamma\beta)}} = \sqrt{\frac{20\times10^{-6}\cdot 400}{6\cdot 108}} = 3.5\,mm$, making the size of the pipe diameter ~ 60 *mm* equal to 17 σ.

The long straight sections connect the ends of the D5O magnets from outside ring to the other side of the interaction region with the D5I inside ring and opposite (as presented in figures bellow).

The ~105*m* long straight pipe of one ring is in the horizontal plane is 35*mm* above the ring plane. The solution is schematically shown in both horizontal and vertical projections in Fig. 10.

The same solution schematically presented in three dimensions is shown in Fig. 11.

Additional drifts to allow the vacuum valves to be placed at the end of the cryostats are provided. At the present triplet cryostat design a distance from the end of the magnetic edge of the quadrupole Q3 to the end of the valve is 2.7059*m*, this is preserved in the present design. The first vertical dipole, as presented in Fig. 10, is connected to that valve. A distance from the magnetic edge of the quadrupole Q1, on the other side of the cryostat, to the flange to connect the present D0 magnet (to be removed in future) is

1.26465*m*. Additional 0.04872*m* are added for a vacuum valve. The second vertical dipole, presented in Fig. 10 is connected to the valve.

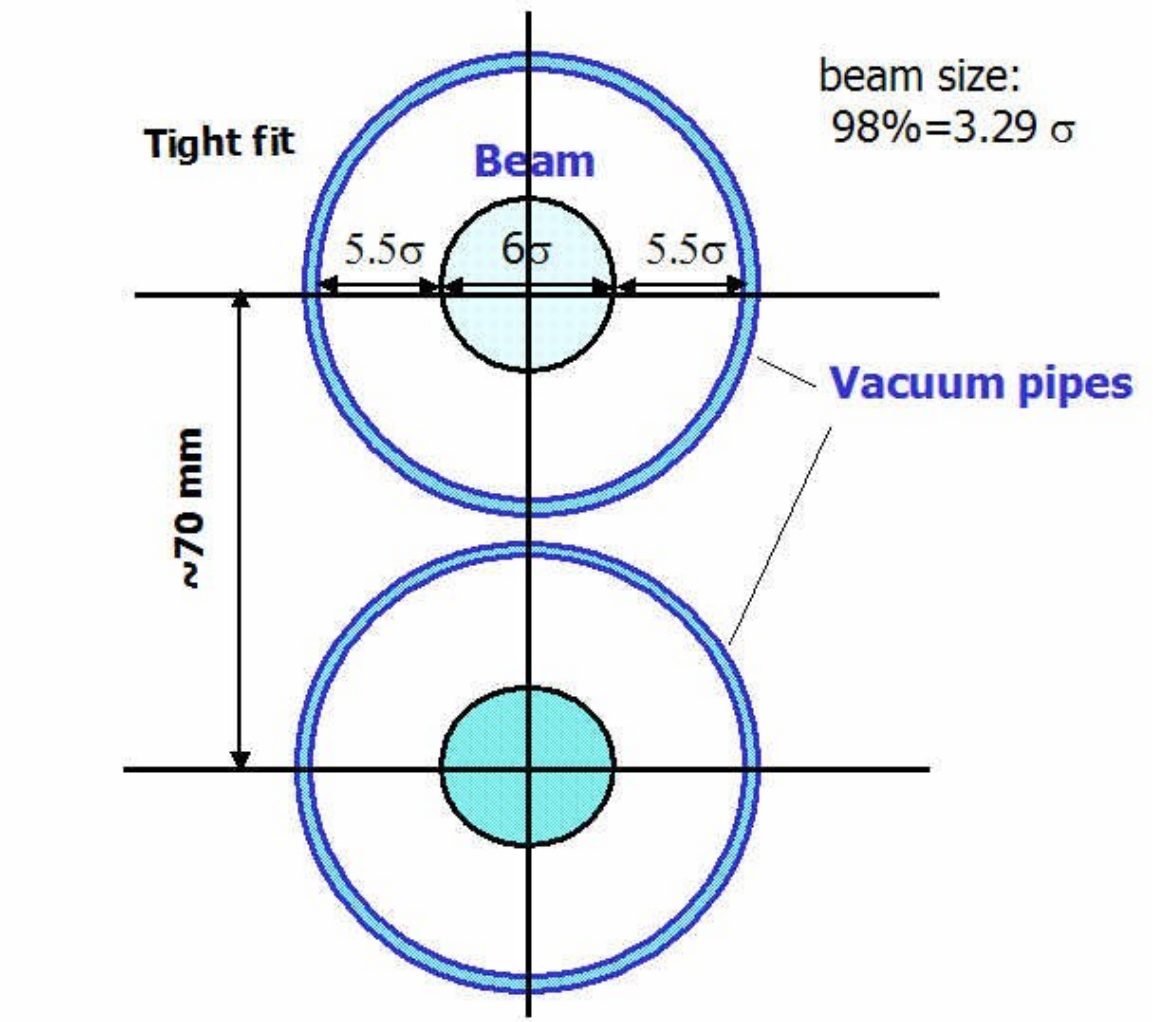

Figure 9: Two vertically separated rings at the crossing point.

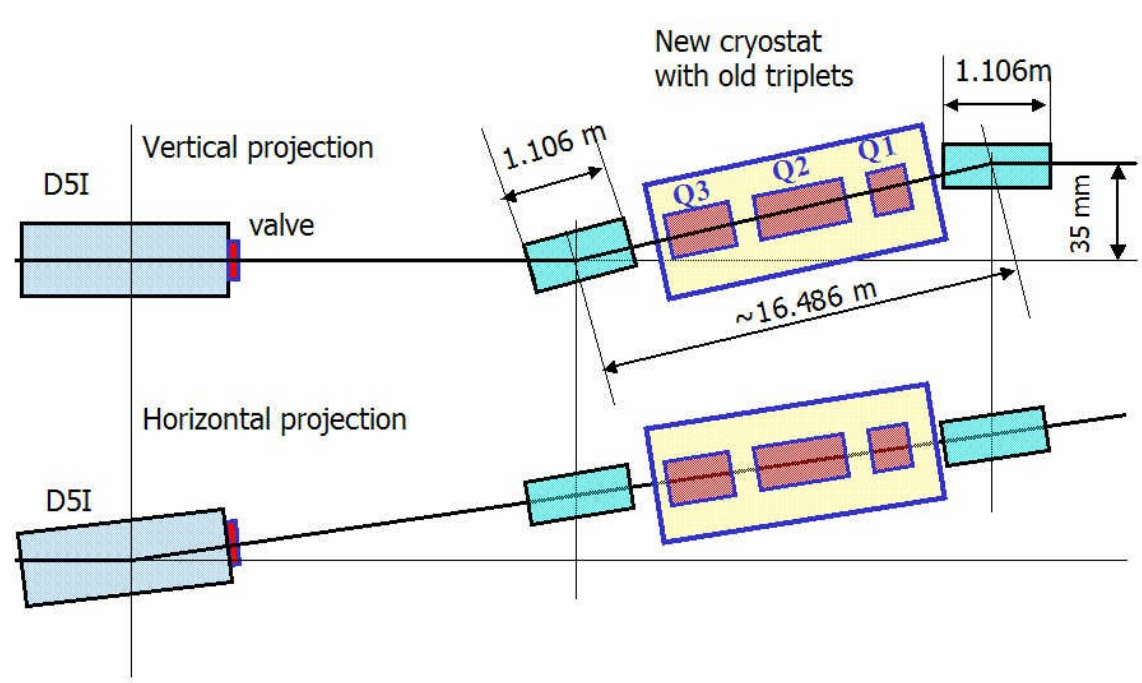

Figure 10: Vertical and horizontal projections of the two rings, schematically presented at one side of the cooling section of the RHIC straight section.

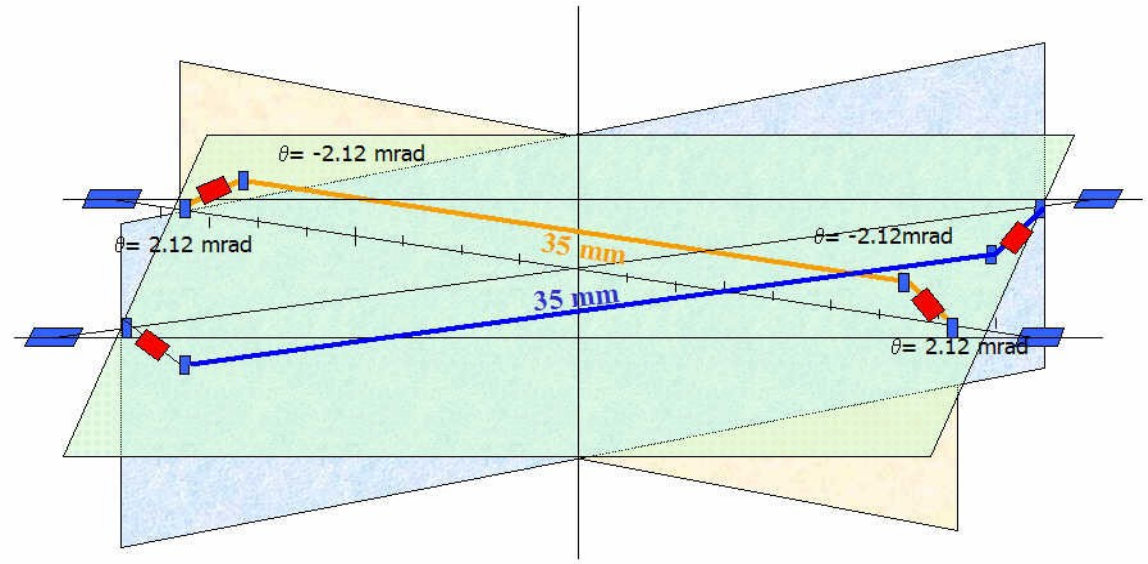

Figure 11: The vertical separation schematically presented in three dimensions.

Design procedure

The required vertical separation or geometrical conditions and the vertical dispersion matching are accomplished without affecting the present horizontal design. The vertical separation of 7 *cm* between the two rings is obtained by L_d=1.101 *m* long warm dipole with magnetic field of B_y=1.6 *T*. All dipoles are the same and provide vertical bending angle of θ=2.124 *mrad* at the maximum energy (Bρ=833.9 *Tm*). The required geometrical condition is schematically presented in Fig. 12.

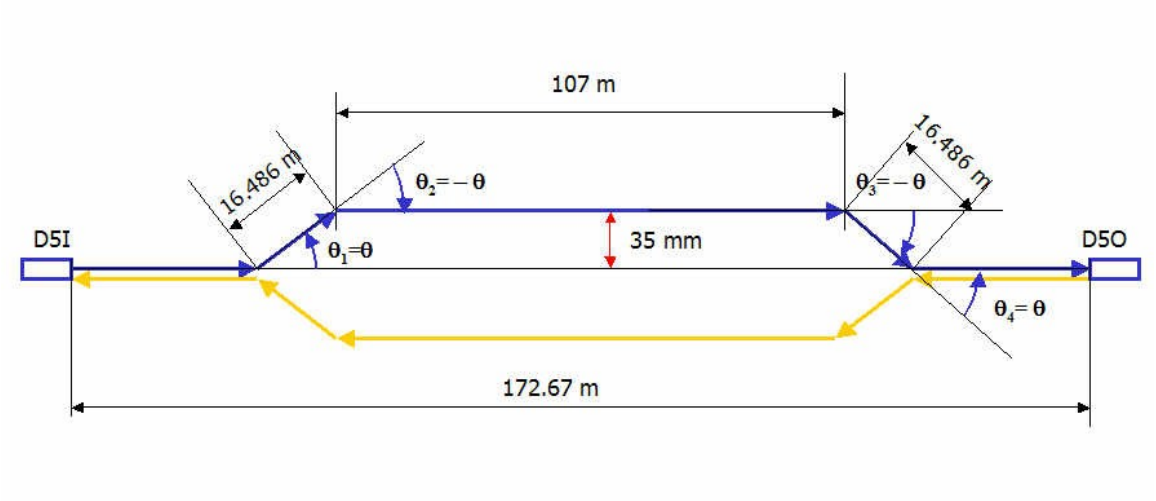

Figure 12: Geometrical constraints.

The vertical dispersion matching was obtained by placement of the vertical dipoles at the lattice positions with the required vertical betatron functions values. First, the second and third vertical dipole are placed as close as possible to the triplet cryostat to allow the longest free space distance between them, making the longest possible cooling section. The design is presented in the normalized dispersion space in Fig 13. The horizontal and vertical axes are defined as:

$$\zeta = D_y \sqrt{\beta_y} + \frac{D_y \alpha_y}{\sqrt{\beta_y}} \quad and \quad \chi = \frac{D_y}{\sqrt{\beta_y}}.$$

The vector ξ_1 is defined $\xi_1 = \theta_1 \sqrt{\beta_1}$, while the betatron phase difference between the two vertical dipoles is presented as angle. The strength of the vector representing the second vertical dipole is related to the strength of the first vector as: ξ_2=0.99407 ξ_1. This is a consequence of the relationship between the vectors presented in Fig. 13.

The matching is achieved by starting from the origin at the end of the last bending dipole labeled as ξ_4. The betatron phase differences between the first and the second dipole and between the second and third dipole are $\phi_{1,2}$=2.48° $\phi_{3,4}$=2.088°, while the phase difference between the second and third dipole is $\phi_{2,3}$= 14.933°.

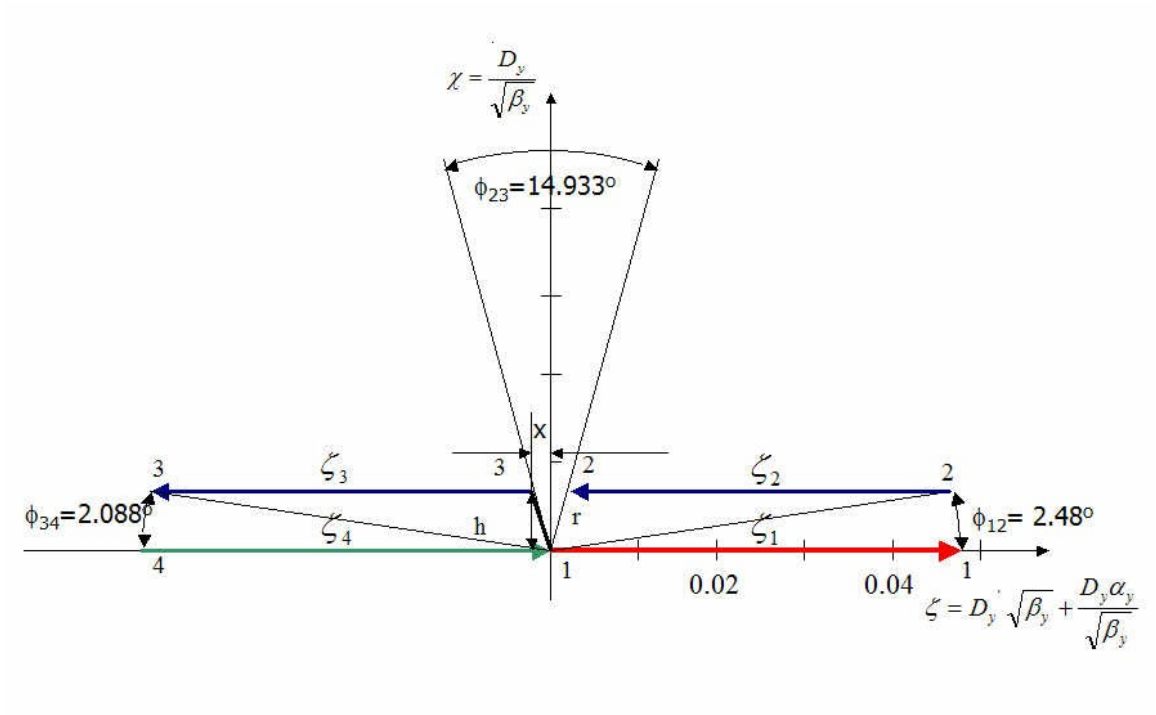

Figure 13: Four vertical dipoles presented in the normalized dispersion space, showing the final result very close to the origin of the graph, indicating excellent dispersion matching.

$$\zeta_4 \cos\phi_{34} = |\zeta_3| + r \sin\frac{\phi_{23}}{2}$$

$$h = \zeta_4 \sin\phi_{34}$$

$$r = \frac{h}{\cos\frac{\phi_{23}}{2}} = \zeta_4 \frac{\sin\phi_{34}}{\cos\frac{\phi_{23}}{2}}$$

$$\zeta_4 = \frac{\zeta_3}{\cos\phi_{34} - \sin\phi_{34} \tan\frac{\phi_{23}}{2}} = 1.00487 \cdot \zeta_3$$

The second vertical dipole has the same bending direction as well as the strength as the third one $\xi_2 = \xi_3$. The position of the first vertical dipole in the lattice should provide matching conditions presented in the next equations:

$$|\zeta_1|\cos\phi_{12} = |\zeta_2| + r\sin\frac{\phi_{23}}{2}$$

$$h = |\zeta_1|\sin\phi_{12}$$

$$r = \frac{h}{\cos\frac{\phi_{23}}{2}} = |\zeta_1|\frac{\sin\phi_{12}}{\cos\frac{\phi_{23}}{2}}$$

$$\zeta_2 = \frac{\zeta_1}{\cos\phi_{12} - \sin\phi_{12}\tan\frac{\phi_{23}}{2}} = 1.00685\cdot\zeta_1$$

The interaction region (IR) for the RHIC cooling is designed as a symmetric solution with respect to the center. The quadrupole triplets on one side of the IR follow the same DFD structure. The regular RHIC lattice is made of anti-symmetric triplets: on one side of there is DFD while on the other is FDF. The horizontal betatron function matching of the RHIC cooling section to the rest of the RHIC lattice is accomplished by adjusting the quadrupole strengths in the interaction region between the triplets and the arc magnets. Due to existing asymmetry the vertical dispersion matching is more difficult. The betatron functions in the interaction region are presented in Table 1.

Table 3. Vertical betatron functions in the cooling interaction region

Element	s(m)	β_y	α_y	ν_y
TLSCI1	83.350	348.251	-10.239	0.583
TLSCI1	83.35	348.251	-10.239	0.583
VKCK1	**86.662**	**412.733**	**-11.1537**	**0.5842**
OQ3Q4	90.693	515.016	-12.47	0.586
Q1I	99.722	381.912	-17.599	0.59
TLSCI1	102.427	407.274	0.135	0.591
VKCK2	**103.092**	**407.1369**	**0.133575**	**0.5911**
MCR	156.522	400	0	0.612
VKCK3	**209.952**	**407.1369**	**-0.133575**	**0.6339**
TLSCO	210.617	407.357	-0.136	0.634
Q3O	222.351	513.876	13.187	0.638
VKCK4	**226.4389**	**411.747**	**11.8701**	**0.6397**
TLSCO1	229.694	338.556	10.687	0.641
TLSCI1	83.35	348.251	-10.239	0.583

Conclusions:

Matching of the vertical dispersion is excellent at the top energy – full cancellation outside of the vertical bending. There will be a small mismatch in the vertical plane from injection to the full energy as the betatron function at the first dipole are not be absolutely the same as after the triplet. The kick size: θ =2.123 *mrad* .The magnetic field assumed B=1.6 *T*, at the full energy Bρ=833.904 *Tm*, the magnetic length required is ~1.106 *m*. There are four dipoles per ring – total of eight dipoles.

References

[1] W. W. MacKay, private communication

[2] T. Roser, private communication

[3] F. Schmidt, http://mad.home.cern.ch/mad/

[4] D. Trbojevic, private communication